Regioselectivity and Network Structure of Difunctional Alkyl-Substituted Aromatic Amine-Based Polybenzoxazines

Hatsuo Ishida* and Daniel P. Sanders

Department of Macromolecular Science, Case Western Reserve University, Cleveland, Ohio 44106-7202

Received November 1, 1999; Revised Manuscript Received August 14, 2000

ABSTRACT: The regioselectivity of the benzoxazine polymerization in aromatic amine-based polybenzoxazines is investigated through systematic manipulation of the monomer chemistry. The network structures of the cured materials are elucidated by FTIR and GC/MS. Selectively protecting or activating sites on the pendant aromatic ring toward electrophilic aromatic substitution with alkyl groups allows a series of materials to be developed which contain a varying amount of phenolic Mannich bridges, arylamine Mannich bridges, and methylene linkages. Activation of sites on the pendant rings by methyl substituent groups lowers the peak exotherm temperature by up to 45 °C. Temperature-modulated differential scanning calorimetry shows that in some of these materials the development of the glass transition temperature exceeds that of the curing temperature.

Introduction

The chemistry of benzoxazines and their oligomeric products has been known for many years.[1−8] Benzoxazines polymerize via a thermally induced ring-opening reaction to form a phenolic structure characterized by a Mannich base bridge (−CH_2−NR−CH_2−), as shown in Scheme 1.[9−11] It has been demonstrated that the preferred reaction site is the position ortho to the hydroxyl functionality on the aromatic ring.[9−14] As polymeric materials, benzoxazines have traditionally been limited to low molecular weight oligomers.[9] Patents by Higginbottom described the initial application of a difunctional benzoxazine monomer.[15,16] Recently, materials with useful mechanical and thermal properties based on benzoxazine chemistry been reported.[17,18] Polybenzoxazines, as a class of thermosetting resins, have been shown to offer a number of useful properties including low melt viscosity, no release of volatiles during cure, no need for harsh catalysts, high glass transition temperature (T_g), high thermal stability, good mechanical properties, and a wide molecular design flexibility.[19−23]

Recently, work has been done to investigate thermal degradation mechanism of these polybenzoxazines.[24,25] It has been shown that the Mannich bridge is the first structure to thermally decompose to release predominantly the primary amine with minor amounts of secondary and other substituted amines as volatiles. A number of degradation schemes have been proposed for both aliphatic[24] and aromatic[25] amine-based benzoxazines. In the case of polybenzoxazines based on Bisphenol A and aniline, analysis of the evolved gases from the thermally degrading resin showed the evolution of a para-methyl-substituted aniline in addition to aniline.[25] To explain the presence of this evolved *p*-toluidine, it has been suggested that the pendant aromatic rings serve as additional sites for polymerization. This proposed mechanism is in agreement with the solid-state ^{13}C and ^{15}N NMR results by Koenig et al.[13,14] It was hypothesized that tethering the Mannich bridge by cross-linking the pendent aromatic ring would stabilize the bridge from thermal degradation. To do so, nitrile, phthalonitrile, and acetylene functionalized anilines have been used in the synthesis of polybenzoxazines.[26−33] These compounds exhibit enhanced char yield and thermal stability over the unfunctionalized arylamine-based materials. Unfortunately, it is still not known to what extent the pendant rings in the unfunctionalized resin are reacted during polymerization. If these rings could be activated toward reaction during curing, the thermal stability of the resin as well as the cross-link density and mechanical properties might be enhanced without the use of the more expensive acetylene, phthalonitrile, or nitrile functionalized anilines.

Scheme 1. Benzoxazine Polymerization

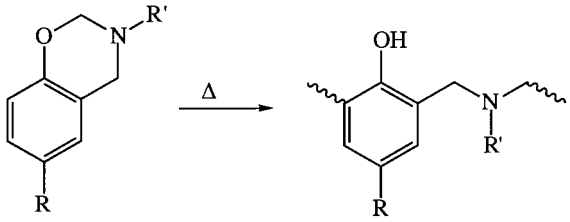

Several groups have attempted to use activation of sites on an arylamine ring to control the regioselectivity of the aminoalkylation reaction.[34−40] In the case of various *N*,*N*-dimethyltoluidines, only the *N*,*N*-dimethyl-*m*-toluidine underwent an aminoalkylation reaction, and the reaction site was the activated para position.[36] This reaction was carried out under less vigorous conditions than was required for the *N*,*N*-dimethylaniline reaction, suggesting that activation of the para position toward the aminoalkylation reaction through the addition of a methyl substituent at the meta position is feasible. Indeed, a previous regioselectivity study by our group has indicated that reaction to the activated sites on the arylamine ring can take place at ordinary curing temperatures.[41] However, significant amounts of bisphenolic and arylamine methylene linkages were generated via a secondary reaction in the compounds activated with methyl substituents at one or both meta positions on the arylamine ring.

This paper will examine the reaction site of the benzoxazine polymerization, and hence the structure of

* To whom correspondence should be addressed.

10.1021/ma991836t CCC: $19.00
Published on Web 10/07/2000

Scheme 2. Benzoxazine Monomer Structures

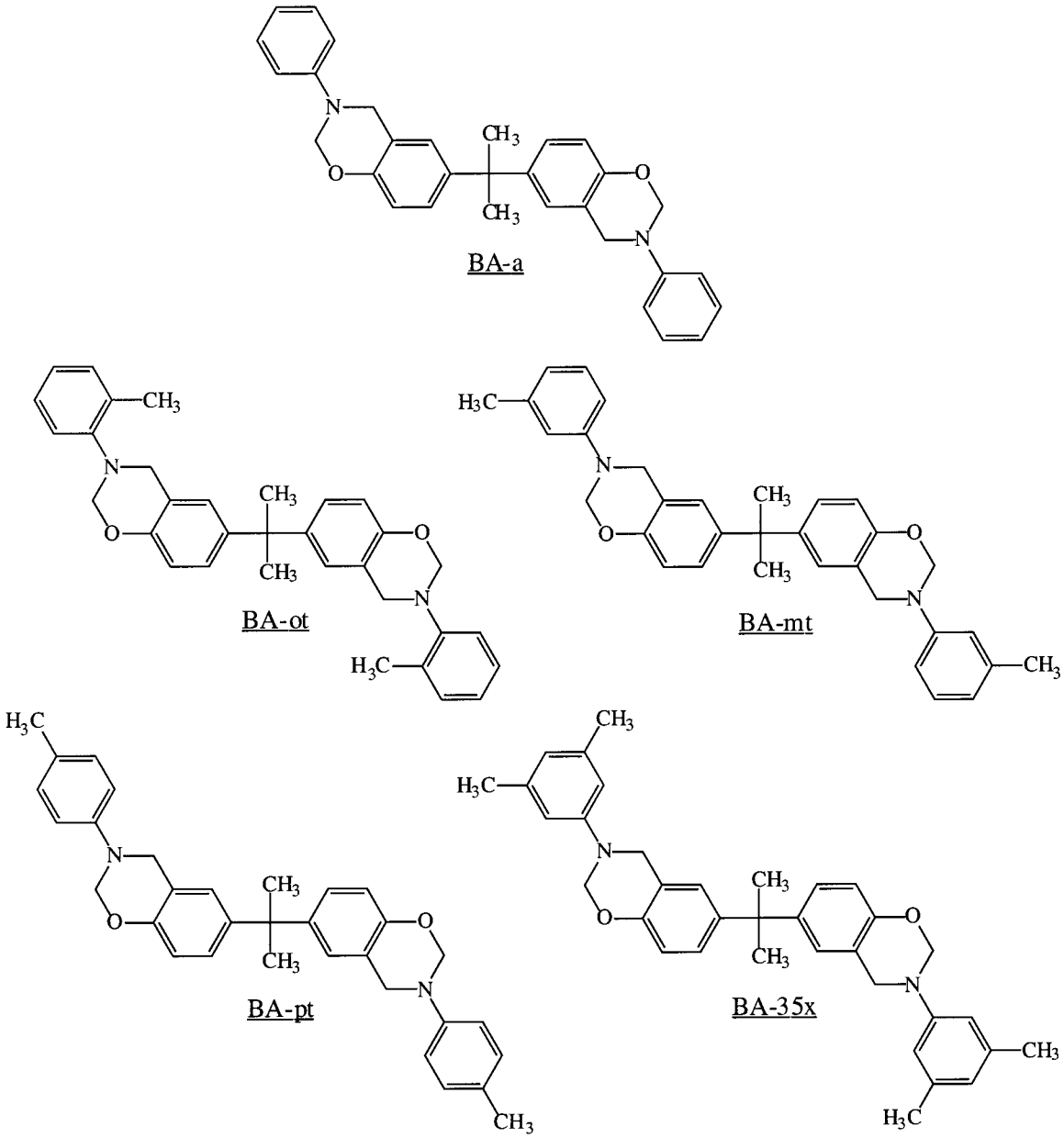

the cured resin, through selective activation and protection of sites on the pendant aromatic ring. Since the previous work examined monofunctional materials which form only low molecular weight oligomers, this paper will investigate the structures produced during cure in a difunctional system capable of cross-linking to form a thermoset network.

Experimental Section

Materials. Difunctional benzoxazine monomers were synthesized from 4,4′-isopropylidenediphenol (Bisphenol A) (Aristech Chemical Co., Polycarbonate grade) and paraformaldehyde (Fluka Chemika, 95%). A series of aromatic amines [aniline (99%), *o*-toluidine (99+%), *m*-toluidine (99%), *p*-toluidine (99%), and 3,5-xylidine (98%)] purchased from Aldrich Chemical Co. were used as received.

Preparation of Benzoxazine Monomers. Difunctional benzoxazines were synthesized via a solventless synthesis method.[18] The Bisphenol A, paraformaldehyde, and arylamine were added to an open container in stoichiometric amounts (1:4:2). The reactants were mixed for 20 min at 120 °C. The crude reaction products were dissolved in diethyl ether and washed with 2 N NaOH solution and rinsed with water. The purified products were dried over sodium sulfate, and the solvent was removed under vacuum. The structures of the benzoxazine compounds are shown in Scheme 2.

6,6′-Bis(3-phenyl-3,4-dihydro-2*H*-1,3-benzoxazinyl)isopropane (BA-a). White powder. ^{1}H NMR ($CDCl_3$, 200 MHz): δ 1.57 ppm (C−CH_3), δ 4.59 ppm (Ar−CH_2−N), δ 5.34 ppm (−O−CH_2−N−), δ 6.5−7.5 ppm (Ar−H). Ring methylene content (−O−CH_2−NR−): 94%. FTIR (KBr): ν 757 and 694 cm^{-1} (monosubstituted benzene); ν 1030 cm^{-1} (C−O str aromatic ether); ν 1232 cm^{-1} (Ar−O−C asym str aromatic C−O); ν 947 cm^{-1} (oxazine ring).

6,6′-Bis(3-(2-methyl)phenyl-3,4-dihydro-2*H*-1,3-benzoxazinyl)isopropane (BA-ot). White powder. ^{1}H NMR ($CDCl_3$, 200 MHz): δ 1.57 ppm (C−CH_3), δ 2.36 ppm (Ar−CH_3), δ 4.36 ppm (Ar−CH_2−N), δ 5.17 ppm (−O−CH_2−N−), δ 6.5−7.5 ppm (Ar−H). Ring methylene content (−O−CH_2−NR−): 83%. Amine methyl content: 82%. FTIR (KBr): ν 760 and 728 cm^{-1} (ortho-substituted benzene); ν 1030 cm^{-1} (C−O str aromatic ether); ν 1232 cm^{-1} (Ar−O−C asym str aromatic C−O); ν 947 cm^{-1} (oxazine ring).

6,6′-Bis(3-(3-methyl)phenyl-3,4-dihydro-2*H*-1,3-benzoxazinyl)isopropane (BA-mt). Light tan powder. ^{1}H NMR

($CDCl_3$, 200 MHz): δ 1.57 ppm ($C-CH_3$), δ 2.31 ppm ($Ar-CH_3$), δ 4.58 ppm ($Ar-CH_2-N$), δ 5.32 ppm ($-O-CH_2-N-$), δ 6.5−7.5 ppm (Ar−H). Ring methylene content ($-O-CH_2-NR-$): 85%. Amine methyl content: 90%. FTIR (KBr): ν 775 and 695 cm^{-1} (meta-substituted benzene); ν 1030 cm^{-1} (C−O str aromatic ether); ν 1232 cm^{-1} (Ar−O−C asym str aromatic C−O); ν 947 cm^{-1} (oxazine ring).

6,6′-Bis(3-(4-methyl)phenyl-3,4-dihydro-2*H*-1,3-benzoxazinyl)isopropane (BA-pt). The reaction was carried out at higher temperature of 135 °C. In addition to purification by washing, BA-pt was able to be recrystallized once from diethyl ether, yielding a white crystalline powder. ^1H NMR ($CDCl_3$, 200 MHz): δ 1.57 ppm ($C-CH_3$), δ 2.26 ppm ($Ar-CH_3$), δ 4.54 ppm ($Ar-CH_2-N$), δ 5.30 ppm ($-O-CH_2-N-$), δ 6.5−7.5 ppm (Ar−H). Ring methylene content ($-O-CH_2-NR-$): 98%. Amine methyl content: 98%. FTIR (KBr): ν 1515 and 808 cm^{-1} (para-substituted benzene); ν 1030 cm^{-1} (C−O str aromatic ether); ν 1232 cm^{-1} (Ar−O−C asym str aromatic C−O); ν 947 cm^{-1} (oxazine ring).

6,6′-Bis(3-(3,5-dimethyl)phenyl-3,4-dihydro-2*H*-1,3-benzoxazinyl)isopropane (BA-35x). Yellowish white powder. ^1H NMR ($CDCl_3$, 200 MHz): δ 1.57 ppm ($C-CH_3$), δ 2.27 ppm ($Ar-CH_3$), δ 4.57 ppm ($Ar-CH_2-N$), δ 5.31 ppm ($-O-CH_2-N-$), δ 6.5−7.5 ppm (Ar−H). Ring methylene content ($-O-CH_2-NR-$): 87%. Amine methyl content: 90%. FTIR (KBr): ν 833 and 695 cm^{-1} (1,3,5-trisubstituted benzene); ν 1030 cm^{-1} (C−O str aromatic ether); ν 1232 cm^{-1} (Ar−O−C asym str aromatic C−O); ν 947 cm^{-1} (oxazine ring).

Characterization. The structure and purity of the monomers were identified via proton nuclear magnetic resonance (^1H NMR) spectroscopy. The NMR was performed on a 200 MHz Gemini ^1H NMR spectrometer. All resonances were referenced with respect to the proton signal of tetramethylsilane (TMS). The purity of the monomers was examined using size exclusion chromatography (SEC) using a Waters 510 HPLC pump with a U6K injector and a Waters 484 tunable absorbance and Waters 410 differential refractive index detectors. The columns were Whatman Styragel 50 nm, 10^2 nm, and 10^3 nm columns. Fourier transform infrared (FTIR) spectra of the monomers were obtained on a Bomem Michelson MB-110 spectrometer with a KBr beam splitter and liquid nitrogen-cooled mercury−cadmium−telluride (MCT) detector. FTIR spectra of the polymerized materials were obtained on a Biorad FTS-60A FTIR spectrometer with a KBr beam splitter and a deuterated triglycine sulfate (DTGS) detector. All spectra were taken of material cast onto KBr plates from chloroform solution at 4 cm^{-1} resolution.

The reaction exotherms of the monomers were measured using differential scanning calorimetry (DSC) with a TA Instruments DSC 2910 high-pressure differential scanning calorimeter. The DSC was pressurized with nitrogen at 2.76 MPa during the run with a slow purge of 50 mL/min. The temperature was ramped at 10 °C/min. The curing reactions were also monitored using a TA Instruments DSC 2920 modulated DSC (MDSC). The temperature was ramped at a linear heating rate of 1.0 °C/min with a superimposed sinusoidal temperature profile with an amplitude of 0.1 °C and a period of 60 s.

The benzoxazine monomers were degassed for 1 h at 110 °C under vacuum before undergoing a step cure in an air-circulating oven. The step profile used to cure samples was as follows: 140 °C, 30 min; 160 °C, 30 min; 170 °C, 45 min; 180 °C, 45 min,; 190 °C, $1^1/_4$ h; 200 °C, $1^1/_2$ h. Glass transition temperatures of the polymerized materials were measured by DSC using a TA Instruments DSC 2920 modulated DSC in standard mode. The temperature was ramped at 10 °C/min. The thermal stability of the cured benzoxazines was measured by thermogravimetric analysis (TGA) using a TA Instruments Hi-Res 2950 thermogravimetric analyzer equipped with a evolved gas analysis (EGA) furnace. The temperature was ramped at 10 °C/min under a nitrogen atmosphere. Evolved gases from the thermally degraded materials were trapped by bubbling the waste gas through HPLC grade chloroform. Mass identification was performed by a Hewlett-Packard 6890 gas chromatograph coupled to a 5973 mass selective detector (GC/MS). The injection port of the GC was held at 250 °C while the GC column was heated from 70 to 280 °C at a heating rate of 8 °C/min. Compounds were tentatively identified using a NIST Mass Spectral Library, Nbs75k. Final assignments were made by injecting solutions of the pure compounds diluted in chloroform. In addition, model polymer systems which decompose to yield target compounds were obtained and degraded in a TGA to produce test samples. Model polymer systems used in this study include polystyrene ($M_w \approx$ 125 00−250 000, Polysciences, Inc.), poly(4-hydroxystyrene) (Hoechst-Celanese), a phenolic resole based on 4-ethylphenol, and a phenolic resole based on 4-isopropylphenol.

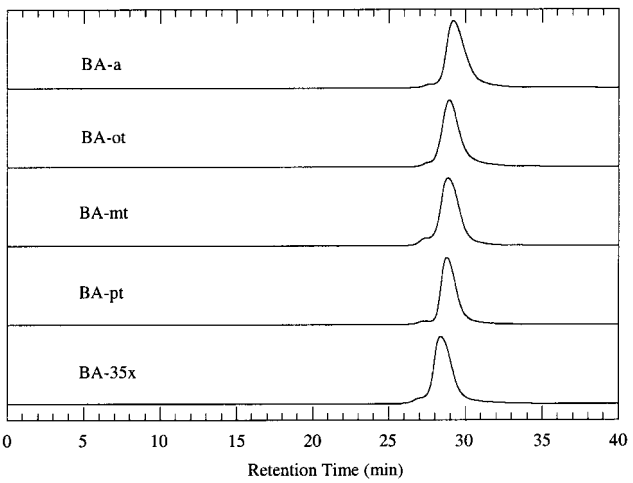

Figure 1. SEC chromatograms of the difunctional benzoxazine monomers.

Results and Discussion

Synthesis. The proton NMR resonances of BA-a have been assigned previously by Liu and Ishida.[42] In addition, the proton NMR resonances of BA-pt and the intermediates and side products of the solventless reaction have been assigned by Liu and Ishida.[36] A resonance appearing near 2.27 ppm is assigned to the methyl protons on the substituted aniline rings. Resonances located near 5.31 and 4.57 ppm are from the methylene protons in the oxazine ring. The absence of significant resonances near 4.1−4.2 and 4.3 ppm indicates that open Mannich base and oligomeric compounds have been removed during the purification procedures. In addition, no resonances at 4.9 ppm corresponding to methylene protons in the triazine intermediate are observed.[42,43] BA-pt has the highest ring content (96%) since it was recrystallized, which eliminated the majority of the single ring compounds. While ring contents in excess of 95% are common for purified difunctional benzoxazines, the materials synthesized using toluidines show slightly lower ring contents. GC/MS analysis of the monomers show that the main impurities are small amounts of open ring phenolic and Schiff base compounds. Since benzoxazine polymerization is acid-catalyzed, it is advantageous to have a few residual phenolic present to initiate polymerization at reasonable temperatures.[41] Since these species have been shown to be generated early on in the polymerization reaction of pure monofunctional benzoxazine monomers,[41] the presence of small amounts of these species will not affect the resulting network structure. The purity of the difunctional compounds is further confirmed by SEC as shown in Figure 1. All compounds show a single peak with a slight shoulder at a shorter retention time. The shoulder is assigned to

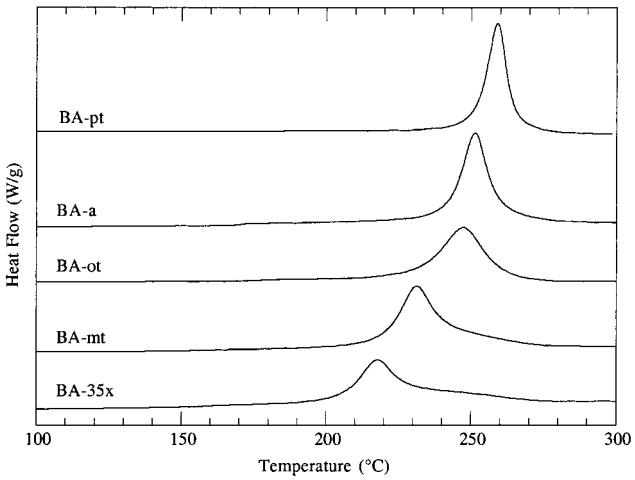

Figure 2. DSC thermograms of the benzoxazine cure.

Table 1. Calorimetric Properties of the Polymerization Reaction

	BA-a	BA-ot	BA-mt	BA-pt	BA-35x
T_g (°C)	168	114	209*	158	243*
exotherm peak (°C)	251	247	231	259	217
heat of reaction (J/g)	340	289	325	310	298

open-ring compounds while the main peak is assigned to the closed-ring compounds.

Polymerization Reaction. The DSC thermograms of the benzoxazine polymerization reactions are shown in Figure 2 and summarized in Table 1. BA-a shows a typical polymerization exotherm for purified difunctional benzoxazines centered at 251 °C. Monofunctional benzoxazine analogues showed similar trends in peak exotherm position.[41] BA-ot shows a much broader exotherm centered at 248 °C as a result of catalytic phenolic groups present. In contrast to the previous compounds, BA-mt and BA-35x exhibit different curing behavior. The shifting of the main polymerization exotherm in BA-mt and BA-35x cannot be explained by either the relative stabilities of the benzoxazine rings toward hydrolysis (both are more stable than BA-a[44]), basicities of the arylamines (*m*-toluidine is nearly the same basicity as aniline[45]), or merely the presence of free phenolic species. Different polymerization kinetics must be taking place in these two compounds.

Benzoxazines with secondary cross-linking mechanisms also show this dual exotherm.[26−33] In the case of acetylene meta-substituted arylamine-based benzoxazines, the curing exotherm is very similar in shape to that of BA-mt and BA-35x; however, it generally occurs at a lower temperature (first exotherm peak around 175 °C).[27] Monofunctional benzoxazine compounds made with nitrile meta-substituted arylamines also showed a peak exotherm temperature of around 236 °C but did not show any type of dual exotherm.[32] Phthalonitrile-based difunctional benzoxazines also showed a decrease in peak exotherm to near 227 °C and exhibited a dual exotherm as the nitrile functionalities polymerize at higher temperatures.[30,31]

Van Mele et al. have pioneered the application of temperature-modulated differential scanning calorimetry (TMDSC) to the polymerization of various thermosetting resins.[46−50] The TMDSC results for the polymerization of BA-a can be seen in Figure 3. A step increase in the heat capacity at around 65 °C indicates the devitrification of the monomer. As the temperature

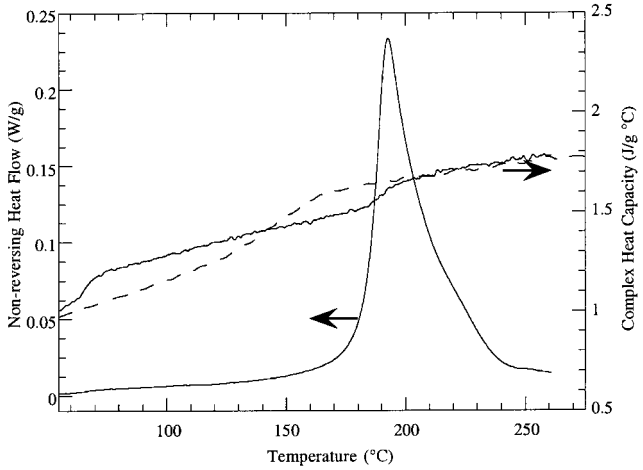

Figure 3. TMDSC thermogram of BA-a cure.

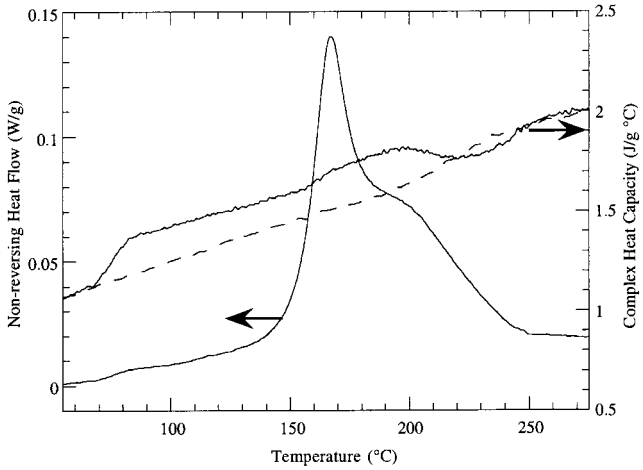

Figure 4. TMDSC thermogram of BA-35x cure.

is ramped, the material begins to polymerize somewhere above 150 °C as evidenced by the exothermic peak in the nonreversing heat flow signal. In accordance with this, a step increase in the heat capacity signal is observed. Upon rerunning the sample after the polymerization was complete, a step increase in the heat capacity signal (the dotted line) can be seen around 150 °C, representing the T_g of the resulting polymer. This result is around 20 °C lower than that seen by either standard DSC or dynamic mechanical analysis (DMA) and is a result of the very slow heating rate employed in the TMDSC measurement. This 20 °C difference is consistent among all samples analyzed by this technique. The TMDSC results for BA-mt are very similar to that of BA-a except that the peak exotherm is around 175 °C instead of 192 °C, and the higher temperature shoulder is much more pronounced in agreement with the previous DSC results. The TMDSC results for BA-35x, as shown in Figure 4, exhibit a new phenomenon. Above 200 °C, the complex heat capacity drops and later recovers at temperatures above 250 °C. Van Mele et al. have assigned this initial step decrease in the heat capacity signal to the vitrification of the reacting system, with the midpoint representing the point where 50% of the material has vitrified.[46−50] The vitrification temperature of 215 °C agrees well with the T_g of this polymer when step cured only up to 200 °C. The recovery in the heat capacity signal represents the devitrification of the reacting system. Clearly, the development of network structure in the substituted and unsubstituted ary-

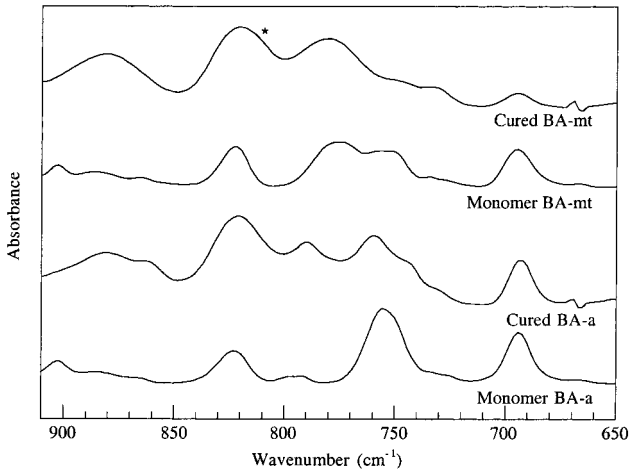

Figure 5. FTIR spectra comparison of cured BA-a and BA-mt.

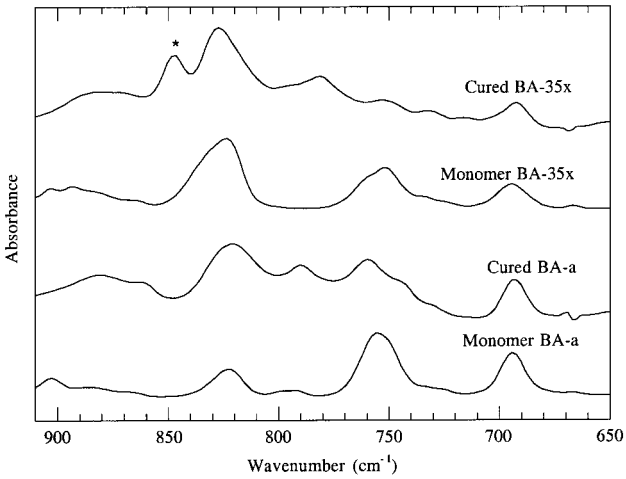

Figure 6. FTIR spectra comparison of cured BA-a and BA-35x.

lamine-based benzoxazines are different. It is suspected that the high-temperature shoulder corresponds to the side reactions which generate the bisphenolic methylene linkages and possibly reaction to the para position of the arylamine ring.[41] Such reactions would not require nearly the same amount of mobility to occur and, therefore, could continue even after the main polymerization reaction becomes diffusion-controlled by the gelation. The development of significant amounts of additional cross-links (i.e., methylene linkages) would increase the T_g of the network significantly. The difference in glass transition temperatures, as shown in Table 1, can be explained by the development of increasing amounts of various methylene and arylamine Mannich base linkages in BA-mt and BA-35x.

Vibrational Analysis. The polymerized structure can be analyzed more thoroughly by FTIR to determine the nature of the polymerization reactions. The infrared vibrational modes of model open-ring benzoxazine structures have been well characterized.[51] The band centered near 947 cm^{-1} associated with the oxazine ring has nearly completely disappeared, indicating a nearly complete loss of the oxazine ring. The bands associated with the aromatic C−O and aromatic ether C−O−C stretches are nearly absent as well. A new band at 1285 cm^{-1} characteristic of a phenolic C−O species arises. In addition, large broad bands centered near 1185 cm^{-1} assigned to the C−N−C asymmetric stretching appear.

The easiest approach to determine which aromatic sites have reacted is to examine the out-of-plane bending modes of the aromatic hydrogens which are more widely separated. A comparison of this region before and after polymerization of BA-a under nitrogen is shown in Figure 5. The bands associated with the five adjacent hydrogen wagging (755 cm^{-1}) and out-of-plane ring bending by sextants (695 cm^{-1}) shift to slightly lower wavenumbers (751 and 694 cm^{-1}, respectively) upon polymerization. The only significant band to develop is centered at 878 cm^{-1}. This band agrees with the frequency predicted for the out-of-plane, out-of-phase hydrogen wagging mode for 1,2,3,5-tetrasubstituted aromatic rings.[52] This is the expected ring substitution if the reaction takes place ortho to the phenolic moiety. BA-mt and BA-35x exhibit slightly different behavior than BA-a. In Figure 5, BA-mt shows the development of a band near 810 cm^{-1} which is very close to where the two adjacent out-of-plane, in-phase hydrogen wagging modes for 3,4-dimethylaniline absorb. This is

Scheme 3. Phenolic Mannich Bridge Network

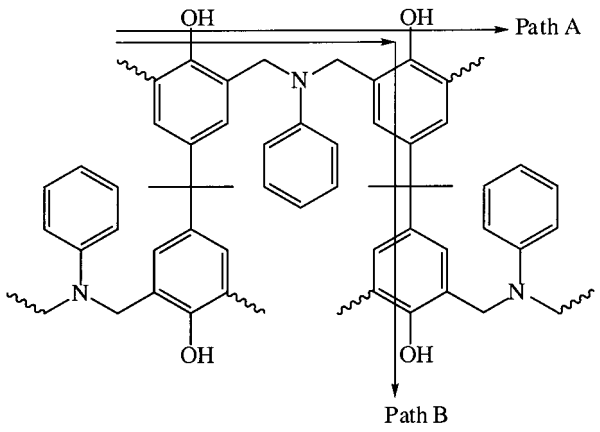

spectroscopic evidence that the pendant arylamine rings activated in the para position can undergo an aminomethylation reaction during the polymerization. To further support this, one can examine the case of BA-35x, shown in Figure 6, which is even further activated. One would expect to find a prominent band near 847 cm^{-1} corresponding to the out-of-plane, in-phase hydrogen wagging mode of the 1,2,3,5-tetrasubstituted arylamine ring.[52] Indeed, a large band centered at 847 cm^{-1} develops after polymerization.

Network Structure. Given the FTIR evidence along with the results of the monofunctional benzoxazine study,[41] a number of possible network structures can be envisioned. If the benzoxazines polymerize only at the ortho phenolic sites, a phenolic Mannich bridge network structure would develop, as shown in Scheme 3. In this structure, two possible main chain pathways can be visualized, both of which include a −C−N−C− Mannich bridge. However, the FTIR data and thermal analysis suggest that some pendant rings react as well. Thus, if one imagines a case in which only these activated sites react and no ortho phenolic positions react, using BA-mt as an example, an arylamine Mannich bridge network structure could form, as shown in Scheme 4. Again two main chain pathways can be visualized. The first, path C, is similar to path B discussed previously. However, a new main chain pathway, path D, exists which proceeds through a −C−N− Mannich bridge through the arylamine ring and then through the next −C−N− Mannich bridge. With

Scheme 4. Arylamine Mannich Bridge Network

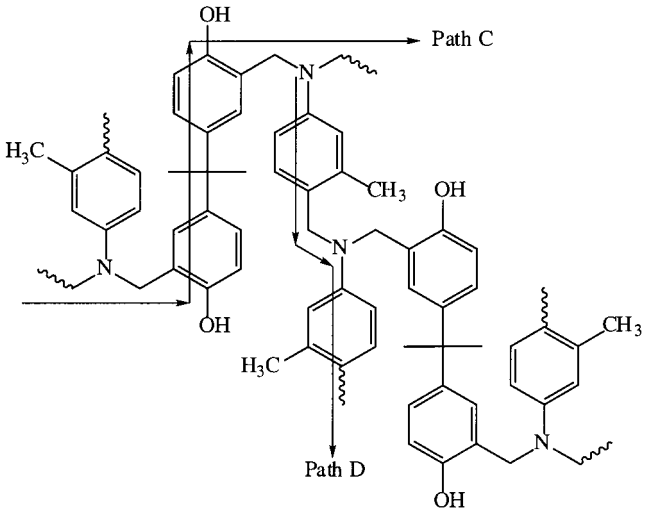

Scheme 5. Bisphenolic Methylene Bridge Network

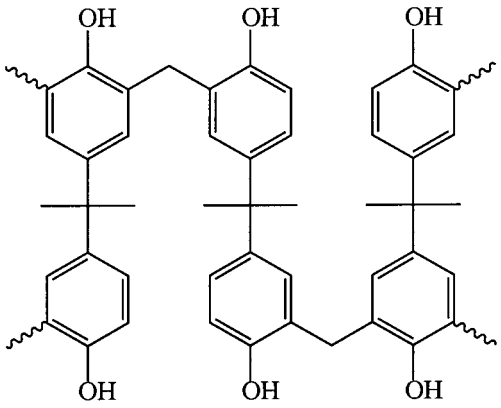

the aromatic carbon−nitrogen bond being significantly stiffened by resonance and the absence of one of the methylene "hinges" in the Mannich bridge, this arylamine Mannich bridge should be significantly more rigid, resulting in a higher T_g at the same extent of conversion.

Given the evidence for various methylene linkages in thermally cured monofunctional benzoxazines, a network in which all of the oxazine rings cleave during cure could produce a fully phenolic network structure shown in Scheme 5. Alternately, if the arylamine ring serves as the site for formation of the methylene linkages, an arylamine methylene bridge network would result, as shown in Scheme 6.

Of course, the actual network structure is expected to be somewhere in the continuum between these four extremes with BA-a and BA-pt being similar to the phenolic Mannich bridge network and BA-mt and BA-35x containing additional amounts of arylamine Mannich bridge and methylene linked structures. For evidence of these network structures, one can examine the NMR spectra of the cured materials to determine exactly the positions of the polymerization reaction. Indeed, solid-state ^{13}C and ^{15}N NMR have been performed on polymerized samples of BA-a. Koenig et al. showed through ^{15}N solid-state NMR that indeed some sites on the arylamine ring do react,[13,14] although they postulated that the predominant site of this side reaction is ortho to the amine substituent rather than para as indicated by the previous FTIR-EGA studies.[25] Koenig et al. also showed that the bisphenolic methylene

Scheme 6. Arylamine Methylene Bridge Network

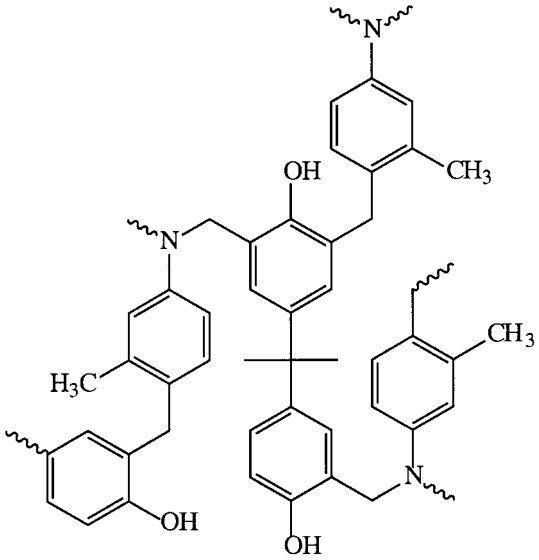

linkage is generated at longer cure times above 200 °C. The previous monofunctional benzoxazine study[41] and additional work by Solomon et al. on the curing of various benzoxazine intermediates based on phenols and hexamethylenetetramine[53−59] showed that such a wide variety of side products were formed during polymerization that structure determination via solid-state NMR is not simple. Instead, the easiest method to determine the local structure of the network is mass spectroscopy. Thermal degradation under an inert environment will fragment the network structure, enabling the initial network structure to be pieced together from the volatilized fragments. This approach has been successfully used to characterize polybenzoxazine thermal degradation mechanisms.[24,25]

Evolved Gas Analysis. The species measured in the GC/MS chromatograms of the solutions containing the collected gases from the series of degraded materials are shown in Table 2. The numeric value corresponds to the percent of mass fragments under the GC chromatogram peak for that fragmented species to the total number of mass fragments from all peaks in the chromatogram. The 35 largest peaks comprised more than 96.9% of the total number of mass fragments in all five materials.

For the phenolic Mannich base network, the pendant arylamine group is the most easily volatilized upon cleavage of the Mannich bridge and, therefore, should be the predominant species in the evolved gases. As degradation proceeds, much smaller amounts of 2-methylphenol, 2,6-dimethylphenol, and other substituted phenols could evaporate upon cleavage of the isopropylene group of the Bisphenol A backbone. Finally, very small amounts of substituted benzene compounds should be released as the char begins to break down.

In an arylamine Mannich bridge network structure, the pendant arylamine group is significantly stabilized. The phenolic portion of the network structure is comparatively less stable now and should make up a larger portion of the evolved species. The most easily volatilized species is a 2-methylphenol species released upon cleavage of the Bisphenol A backbone. In addition, a significant amount of the amine compound released should be substituted by methyl groups on the activated sites.

Table 2. GC/MS Analysis of Network Fragments

retention time (min)	evolved species	parent ion (*m*/*z*)	assigned[a]	BA-a	BA-ot	BA-mt	BA-pt	BA-35x
2.54	toluene	92	L,M,N	1.61	0.83	1.38	1.10	0.59
3.51	*p*-xylene	106	L,M,N	0.13	0.06	0.16	0.09	0.06
3.61	*m*-xylene	106	L,M,N	1.00	1.03	1.44	1.57	1.18
3.90	styrene	104	M,N	0.05	0.04	0.10	0.06	
3.94	ethylbenzene	106	M,N	0.07	0.10	0.35	0.06	0.16
4.99	3-ethyltoluene	120	M,N	0.18	0.22	0.32	0.30	0.21
5.10	1,3,5-trimethylbenzene	120	M,N	0.18	0.20	0.28	0.27	0.45
5.18	phenol	94	L,M,N	8.00	5.42	6.90	7.81	5.68
5.25	aniline	93	L,M,N	57.18	0.51		1.04	
5.54	1,2,4-trimethylbenzene	120	M,N	0.04	0.09	0.26	0.09	0.55
5.61	2,3-benzofuran	118	M,N	0.30	0.31	0.26	0.35	0.28
6.52	*o*-cresol	108	L,M,N	11.60	11.86	15.16	13.15	19.57
6.68	1-ethyl-3,5-dimethylbenzene	134	N,P	0.09	0.10	0.20	0.13	0.20
6.81	*n*-methylaniline	107	L,M,N	2.28				
6.87	*p*-cresol	108	L,M,N	1.53		1.38	1.90	0.84
6.96	*p*-toluidine	107	L,M,N	5.01		1.16	53.25	0.59
6.99	*o*-toluidine	107	M,N		60.44			
7.04	*m*-toluidine	107	M,N			52.81		
7.44	7-methyl-2,3-benzofuran	132	N	0.30	0.56	0.42	0.40	0.75
7.54	2,6-dimethyl phenol	122	L,M,N	3.28	5.49	5.85	4.43	11.92
7.63	4-methyl-2,3-benzofuran[b]	132	N	0.13	0.18		0.15	
8.05	2-ethylphenol	122	N,P	0.50	0.51	0.45	0.59	0.49
8.25	2,4-dimethylphenol	122	M,N	1.27	1.64	1.50	1.70	1.86
8.51	*N*-methyl-*o*-toluidine	121	M,N		1.59	0.15		
8.56	*N*-methyl-*p*-toluidine	121	M,N				3.09	
8.58	4-ethylphenol	122	M,N,P	0.65	0.74	0.39		0.30
8.62	*N*-methyl-*m*-toluidine	121	M,N			2.40		
8.67	2,4-dimethylaniline	121	M,N	0.32	2.32		1.46	
8.76	2,5-dimethylaniline	121	M,N			1.35		
8.82	3,5-xylidine	121	M,N	0.09	0.10	0.55	0.19	45.27
8.96	2-ethyl-4-methylphenol	136	N,P	0.20	0.31	0.29	0.32	0.94
9.22	3,4-dimethylaniline	121	M,N			0.63		
9.31	2,4,6-trimethylphenol	136	M,N	0.22	0.41	0.85	0.35	0.63
9.44	4,7-dimethyl-2,3-benzofuran[b]	145/6	N,P	0.09	0.14	0.10	0.10	0.14
9.66	4-isopropylphenol	136	M,N,P	0.83	0.65	0.59	0.83	0.45
9.88	4-ethyl-2-methylphenol	136	N,P	0.59	0.92	0.57	0.83	0.80
10.33	*N*-methyl-3,5-xylidine	135	M,N	0.10	0.13			1.69
10.89	2-methyl-4-isopropylphenol	150	N,P	1.12	1.22	1.09		1.61
11.03	3,4,5-trimethylaniline	135	N					1.30
11.50	2,3,5-trimethylaniline	135	N					0.21
11.82	2,6-dimethyl-4-isopropylphenol	164	N,P	0.18	0.42	0.23	0.23	0.66
total				99.12	98.46	99.57	96.92	99.38

[a] Assignments confirmed by L = literature, M = model compound, N = NIST MS library, P = degraded model polymer. [b] Probably 5-methyl substituted but only 4-methyl substituted species are available in the NIST database.

Finally, in the bisphenolic methylene bridged structures, most free amine species will have volatilized during the curing process, and therefore, primarily phenolic compounds with some substituted amines will be released upon thermal degradation. In the arylamine methylene structures, all amines volatilized will have additional substitutions. In both methylene bridged structures, the amount of dangling unreacted Mannich, *N*-methyl Mannich, and Schiff bases will be significantly reduced, resulting in the evolution of less primary amine and *N*-methylamine.

The network structure of BA-a seems to be very much like that of the phenolic Mannich bridge structure since the free aniline is by far the most dominant species released. For BA-pt, the free amine concentration is very similar to that of BA-a, but the amounts of 2-methylphenol and 2,6-dimethylphenol released are slightly larger. These two compounds have similar network structures based upon this analysis. Both are primarily phenolic Mannich bridge network structures with a small amount of the pendant rings being tethered.

BA-ot shows the most free amine species in the evolved gases. The steric hindrance and electronic effects generated by the presence of a bulky methyl group ortho to the amine hinders effective polymerization of the oxazine ring. In this network structure, there are likely a considerable number of dangling Mannich bases that are easily volatilized.

As the activation of the para positions of the arylamine ring increases, the amount of free amine volatilized decreases. In addition, the amount of 2-methylphenol released rises significantly. This indicates that less ortho phenolic positions have reacted. This may be due to the site of polymerization shifting toward activated sites on the arylamine ring. The amount of 2,6-dimethylphenol also rises as the activation of the arylamine ring positions are increased. However, previous work[41] has indicated that larger number of oxazine rings degrade during the cure of the compounds with the more activated arylamine rings to produce more methylene linkages. BA-mt and BA-35x, therefore, appear to have more phenolic and arylamine methylene bridge and arylamine Mannich bridgelike network content than the other compounds.

To examine other possible polymerization sites, one can examine the substituted amine compounds released. For BA-mt, the 4, 5, and 6 positions appear to have reacted. It is interesting to note that the reaction at position 6 (2,5-dimethylaniline) is more predominant than at position 4 (3,4-dimethylaniline), in contrast to

the studies of Miocque et al.[36] In the case of BA-35x, the 4 position dominates over the more sterically hindered 2 position. It is interesting to note that the total relative amount of reacted arylamine rings is highest in BA-a as indicated by the GC/MS results. Unfortunately, reacting to sites on the arylamine ring during the polymerization will also increase the chances of the amine being trapped in the char to form heterocyclic and other char structures during thermal degradation. Considering the T_g of the cured materials, it is unlikely that BA-a reacts more at arylamine sites than BA-mt and BA-35x.

Contrary to expectations, the evolution of 1,2,4-trimethylbenzene species is also observed. This indicates that the position meta to the phenolic species (para to the original oxazine ring methylene) also reacts. The meta position has been shown to react, albeit at higher curing temperatures and longer curing times.[60] The amount of 1,2,4-trimethylbenzene evolved is similar in BA-a, BA-ot, and BA-pt; however, it increases significantly in BA-mt and BA-35x. If this site has reacted during the polymerization, 2,3,4-trimethylphenol and/or 2,3,4,6-tetramethylphenol should be observed in the evolved gases; however, these compounds were not detected. Therefore, reaction at the meta-phenolic sites might occur only during char formation at higher temperatures and not during the polymerization reaction. The larger number of these species being formed in the case of BA-mt and BA-35x is not surprising given polymerized benzoxazine compounds made with those amines having much greater extents of formation of bisphenolic methylene linkages.[41] Other products of char formation reactions were also observed such as various substituted 2,3-benzofuran species. In addition, 2-ethylphenol was observed in nearly the same concentration in all five materials. Solomon et al. have observed an ethylene-bridged bisphenolic species in the curing of phenolic resins and have hypothesized a mechanisms for their formation.[53−59] This species could be a predecessor of the 2,3-benzofuran species during thermal degradation.

Significant amounts of styrene were detected in the evolved gases; however, no 4-hydroxystyrene was observed. This indicates that the release of styrene occurs during the latter stages of thermal degradation as the cross-linked char begins to break down rather than during the initial cleavage of the Bisphenol A backbone around 400 °C. Previous thermal degradation studies have suggested the presence of an isocyanobenzene derivative in the evolved gases of BA-a.[25] This species was not observed in this work; however, 3-ethyltoluene was observed which elutes at nearly the same retention time.

Previous work has suggested the formation of amide and imide species in the network structure due to the oxidation of the Mannich bridges during the high-temperature cure.[25] A model aromatic amide compound, poly(*p*-phenylene terephthalamide), degrades under nitrogen to release primarily aniline and benzonitrile. Very minute amounts of benzonitrile were identified in the evolved gases of BA-a. However, the quantities released were so small that they cannot be considered to be definitive evidence for the hypothesized amide and imide structures.

Conclusions

A series of benzoxazine resins have been synthesized which upon polymerization contain a varying amount of phenolic Mannich bridge, arylamine Mannich bridge, and methylene bridge structures. These thermally polymerized Bisphenol A based benzoxazines contain no reactive functionalities on the arylamine group. The network structure of these aromatic amine-based polybenzoxazines has been tailored through systematic manipulation of the monomer chemistry. Activation of sites on the pendant rings by methyl substituent groups lowers the peak polymerization exotherm temperature by as much as 45 °C. GC/MS analysis of the degraded materials indicates that in BA-a, BA-ot, and BA-pt the network structure consists of largely phenolic Mannich base structures with a small amount of the arylamine rings being cross-linked by Mannich bridges. The network structures of BA-mt and BA-35x also contain increasing amounts of methylene-bridged species in the network structure which give rise to significantly enhanced glass transition temperatures.

Acknowledgment. This material is based upon work supported under a National Science Foundation Graduate Fellowship. The authors gratefully acknowledge the partial financial support of the NSF Center for Molecular and Microstructure of Composites (CMMC) which is jointly sponsored by the State of Ohio and the Edison Polymer Innovation Corporation (EPIC), representing industrial members.

References and Notes

(1) Holly, F. W.; Cope, A. C. *J. Am. Chem. Soc.* **1944**, *66*, 1875.
(2) Burke, W. J.; Weatherbee, C. *J. Am. Chem. Soc.* **1950**, *72*, 4691.
(3) Burke, W. J.; Stephens, C. W. *J. Am. Chem. Soc.* **1952**, *74*, 1518.
(4) Burke, W. J.; Murdoch, K. C.; Ec, G. *J. Am. Chem. Soc.* **1954**, *76*, 1677.
(5) Burke, W. J. *J. Am. Chem. Soc.* **1949**, *71*, 609.
(6) Lane, E. S. U.K. Pat. 694.489, 1953.
(7) Schreiber, H. German Offen, 2,255,504, 1973.
(8) Schreiber, H. German Offen, 2,323,936, 1973.
(9) Reiss, G.; Schwob, J. M.; Guth, G.; Roche, M.; Lande, B. In *Advances in Polymer Synthesis*; Culbertson, B. M., McGrath, J. E., Eds.; Plenum: New York, 1985; pp 27−49.
(10) Burke, W. J.; Bishop, J. L.; Glennie, E. L.; Bauer, W. N., Jr. *J. Org. Chem.* **1965**, *30*, 3423.
(11) Burke, W. J.; Glennie, E. L.; Weatherbee, C. *J. Org. Chem.* **1964**, *29*, 909.
(12) Burke, W. J.; Smith, R. P.; Weatherbee, C. *J. Am. Chem. Soc.* **1952**, *74*, 602.
(13) Russell, V. M.; Koenig, J. L.; Low, H. Y.; Ishida, H. *J. Appl. Polym. Sci.* **1998**, *70*, 1401.
(14) Russell, V. M.; Koenig, J. L.; Low, H. Y.; Ishida, H. *J. Appl. Polym. Sci.* **1998**, *70*, 1413.
(15) Higginbottom, H. P. U. S. Pat. 4,501,864, 1985.
(16) Higginbottom, H. P. U. S. Pat. 4,557,979, 1985.
(17) Ning, X.; Ishida, H. *J. Polym. Sci., Part B: Polym. Phys.* **1994**, *32*, 921.
(18) Ning, X.; Ishida, H. *J. Polym. Sci., Part A: Polym. Chem.* **1994**, *32*, 1121.
(19) Liu, J.; Ishida, H. In *Polymeric Materials Encyclopedia*; Salamone, J. C., Ed.; CRC Press: New York, 1996; pp 484−494.
(20) Shen, S.; Ishida, H. *J. Appl. Polym. Sci.* **1996**, *61*, 1595.
(21) Shen, S.; Ishida, H. *Polym. Comput.* **1996**, *17*, 5, 710.
(22) Allen, D. J.; Ishida, H. *J. Polym. Sci., Part B: Polym. Phys.* **1996**, *34*, 1019.
(23) Low, H. Y.; Ishida, H. *Macromolecules* **1997**, *30*, 1099.
(24) Low, H. Y.; Ishida, H. *J. Polym. Sci., Polym. Phys.* **1998**, *36*, 1935.
(25) Low, H. Y.; Ishida, H. *Polymer* **1999**, *40*, 4365.
(26) Low, H. Y.; Ishida, H. *J. Polym. Sci., Part B: Polym. Phys.* **1999**, *37*, 647.
(27) Kim, H. J.; Brunovska, Z.; Ishida, H. *Polymer* **1999**, *40*, 6565.
(28) Kim, H. J.; Brunovska, Z.; Ishida, H. *Polymer* **1999**, *40*, 1815.
(29) Kim, H. J.; Brunovska, Z.; Ishida, H. *J. Appl. Polym. Sci.* **1999**, *73*, 857.

(30) Kim, H. J.; Brunovska, Z.; Ishida, H. *Polymer* **1999**, *40*, 6565.
(31) Brunovska, Z.; Ishida, H. *Thermochim. Acta* **2000**, *357*, 195.
(32) Brunovska, Z.; Lyon, R.; Ishida, H. *Thermochim. Acta* **2000**, *357/358*, 195.
(33) Brunovska, Z.; Ishida, H. *J. Appl. Polym. Sci.* **1999**, *73*, 2937.
(34) Miocque, M.; Vierfond, J.-M. *Bull. Soc. Chim. Fr.* **1970**, *5*, 1896.
(35) Miocque, M.; Vierfond, J.-M. *Bull. Soc. Chim. Fr.* **1970**, *5*, 1901.
(36) Miocque, M.; Vierfond, J.-M. *Bull. Soc. Chim. Fr.* **1970**, *5*, 1910.
(37) Tsuchida, E.; Tomono, T. *J. Polym. Sci., Part A: Polym. Chem.* **1973**, *11*, 723.
(38) Tsuchida, E.; Hasegawa, E.; Tomono, T. *J. Polym. Sci., Part A: Polym. Chem.* **1974**, *12*, 953.
(39) Tsuchida, E.; Hasegawa, E.; Tomono, T. *J. Polym. Sci., Polym. Lett.* **1974**, *12*, 139.
(40) Tsuchida, E.; Hasegawa, E. *J. Polym. Sci., Polym. Lett.* **1976**, *12*, 103.
(41) Ishida, H.; Sanders, D. P. *Polymer*, in press.
(42) Liu, J. Ph.D. Thesis, Case Western Reserve University, 1995.
(43) Brunovska, Z.; Liu, J. P.; Ishida, H. *Macromol. Chem. Phys.* **1999**, *200*, 1745.
(44) Moloney, G. P.; Craik, D. J.; Iskander, M. N. *J. Pharm. Sci.* **1992**, *7*, 692.
(45) Morrison, R. T.; Boyd, R. N. *Organic Chemistry*, 6th ed.; Prentice Hall: Englewood Cliffs, NJ, 1992; pp 850−3.
(46) Van Asche, G.; Van Hemelrijck, A.; Rahier, H.; Van Mele, B. *Thermochim. Acta* **1996**, *286*, 209.
(47) Van Asche, G.; Van Hemelrijck, A.; Rahier, H.; Van Mele, B. *Thermochim. Acta* **1997**, *304/305*, 209.
(48) Van Hemelrijck, A.; Van Mele, B. *J. Therm. Anal.* **1997**, *49*, 437.
(49) Van Asche, G.; Van Hemelrijck, A.; Rahier, H.; Van Mele, B. *Thermochim. Acta* **1995**, *268*, 121.
(50) Swier, S.; Van Asche, G.; Van Hemelrijck, A.; Rahier, H.; Verdonck, E.; Van Mele, B. *J. Therm. Anal.* **1998**, *54*, 585.
(51) Dunkers, J.; Ishida, H. *Spectrochim. Acta* **1995**, *51A*, 5, 855.
(52) Colthup, N. B.; Daly, L. H.; Wieberly, S. E. *Introduction to Infrared and Raman Spectroscopy*, 3rd ed.; Academic Press: New York, 1990.
(53) Dargaville, T. R.; De Bruyn, P. J.; Lim, A. S. C.; Looney, M. G.; Potter, A. C.; Solomon, D. H.; Zhang, X. *J. Polym. Sci., Part A: Polym. Chem.* **1997**, *35*, 1389.
(54) Zhang, X.; Looney, M. G.; Solomon, D. H.; Whittaker, A. K. *Polymer* **1997**, *38*, 5835.
(55) Zhang, X.; Potter, A. C.; Solomon, D. H. *Polymer* **1998**, *39*, 399.
(56) Zhang, X.; Solomon, D. H. *Polymer* **1998**, *39*, 405.
(57) Zhang, X.; Potter, A. C.; Solomon, D. H. *Polymer* **1998**, *39*, 1957.
(58) Zhang, X.; Potter, A. C.; Solomon, D. H. *Polymer* **1998**, *39*, 1967.
(59) Zhang, X.; Solomon, D. H. *Polymer* **1998**, *39*, 6153.
(60) Cid, J. A. Ph.D. Thesis, Case Western Reserve University, 1996.

MA991836T